Influence of six-step heat treatment on microstructures and mechanical properties of 5160 alloy steel

Pattama APICHAI[1,*]

[1]*Department of Physics, Faculty of Science, Lampang Rajabhat University, Muang Lampang, Lampang, 52100, Thailand*

Corresponding author e-mail: pattama.apic@lpru.ac.th

Abstract

AISI 5160 alloy steel grade with complete martensite structure to get the high-strength steel sheets quenched at 900 (Q1), 870 (Q2), 840 (Q3) and 810°C (Q4), respectively and temped at 780°C (Q5) and 680°C (Q6), respectively. The results show ferrite and pearlite microstructural appeared in as-sheet conditions. The strengthening rarely increased with increasing heat treatment steps, while the percentage elongation gradually decreased. The hardness change was secure with that of strengthening for the quenched martensite. In contrast, differences between the initial martensite hardness were no noticeable changes. The Q4 hardening involved the peak hardness and maximum ultimate tensile strength due to carbide distribution in the martensite matrix. The coarse ferrite grains have occurred after Q5 cause significantly reduced hardness and tensile strength. However, the percentage elongation increased with increasing quenching step to Q5 hardening. The excellent 5160 steel performed by Q6 hardening characteristic gained most hardness, ultimate tensile strength, and elongation approximately 60 HRC, 835 MPa, and 12.09%, respectively. Martensite structure transformed to among carbide distribution tempered martensite matrix.

1. Introduction

Automotive components manufacturers use high carbon and chromium steel, AISI 5160 grade, in leaf and coil springs. Because of their outstanding toughness, increased flexibility, and excellent fatigue resistance [1], they attributed the benefits of alloy steel to optimizations. The development in structural applications of alloy steels consists of two-stage work hardening [2-3]. The process starts with a partial or complete austenitization followed by rapid cooling.

The temperature between martensite starts and finishes to obtain a controlled amount of martensite. Hardened and tempered application steels are widely using to allow constitutions with material exhibits appropriate for their attended benefit. Iron-carbon alloy heated to their suitable quenching temperature, usually between 780°C to 900°C. Accordingly, the instances were tempered at 180°C to 450°C to procure the optimized combining quality of being physically strong, flexible, and challenging [4]. However, the veritable states' development for all three steps was definitely by steel composition, constitutive size, and the properties demanded. In carbon steel, the FCC initial γ-austenite phase mainly was commuting into the BCT α′-martensite structure. Phosphorous was estimated to encourage α′-martensitic reformation and to enlarge the α′-martensite feature heat [5]. The findings enable predicting compounding elements on the form and phase reorganization emerging during deformity in steels. The homogeneous and equal recrystallized austenitic microstructures occurred after heating at 1100°C for 30 min [6]. Developing a new processing technology was controlled-rolled at 1050, 850, 800, 750, and 700°C to get high-strength alloy steel.

Tempering was condition prehistory participated with the especially in the metallurgy of martensite in steels. It illustrated how the structure and material exhibit upon the application of forces change. The metastable specimens carried isothermally at heating, where γ-austenite not be able to uniform. The varies throughout the temped of α′-martensite can be categorized into compasses. Total carbon in drawbacks solid solution differentiates or manners clusters insides the reliable solution during the first stage. There consequently precipitates as cementite in low-carbon steels and iron-carbides transition in high-carbon alloys. The carbon is absorbed in the solid solution, remarkable if the residue was a metamorphosis carbide.

Almost all of the excess carbon precipitated was expanding during two/annealing steps and the carbides whole transform into increasingly steady Fe_3C. Retained austenite would analyze during this step. The crystallographic defect carbide's roughening was recrystallization into coased grains during three/tempering steps [7]. Zhou *et al.* [8] investigated processed in three steps, intercritical anealing at 780°C for 30 min, intercritical tempering at 660°C for 30 min, and tempering at 500°C for 30 min in low carbon steel. The primary α-ferrite retained austenite, and a small amount of bainite-martensite has occurred. Xie *et al.* [9] reported that low alloy steels have regular yield strengths of less than 460 MPa in the first steps. And coherently advanced overall percentage elongations, second-step alloy steels have great yield strength up to 1000 MPa but down flexibility.

However, three-step alloy steels concurrently overacting improve yield strength to 800 MPa and outstanding elasticity, with a total percentage elongation identical to the first step. The initiated crack in α′-martensite determines a mobilized stress/strain field, resulting

in an elevated stress/strain in the near ferrite structure. Additionally, high-strength deformation is stored, primary elasticity force can be disconnect ever the crack begins disseminating, resulting in unsteady crack outgrowth [10].

Novel strength steel was composed of multi-heated martensite with different stabilities. Nevertheless, α′-martensitic transforms were a significant spectacle that influenced their application used properties and studied uproariously. As an ongoing requirement for developing 5160 sheets of steel, this offers an advanced federation of excellent strength and great elasticity. As shown in this paper, intellect the α′-martensitic transformation model has received larges of integration. Multi-steps were introduced in prising carbides of intermetallics distributed compounds and Cu carbide precipitates in 5160 alloy steel sheets. The precipitation strengthening relationships of multi-heat treatment alloys have also discoursed.

2. Procedures

2.1 Materials and methods

A hot-rolled sheet AISI-5160 alloy steel sheet with 1.20 cm × 6 cm × 102 cm dimension was used as the as-sheet metal. The chemical element constituent of the 5160-steel was allowed 0.58 wt% C, 0.23 wt% Si, 0.77 wt% Mn, 0.02 wt% P, 0.01 wt% S, 0.73 wt% Cr, 0.04 wt% Ni, 0.03 wt% Cu, and 0.01 wt% V in Fe balance. The multi-heat treatment is compounded of strength-hardening, forwarded by quenched in different media. The heat treatments defined hardening at 900 (Q1), 870 (Q2), 840 (Q3), and 810°C (Q4), respectively, followed by tempering at 780°C (Q5) and 680°C (Q6), respectively, in the experimental procedures. The step-heat treatment conditions and corresponding specimen codes were enumerated schematically in Figure 1. Three types of quenching media, water at room temperature, oil in the air, and brine at 200°C, were used to quench the samples.

2.2 Characterization

The as-sheet and heat-treated 5160 specimens were cut to be a diameter of 2 cm^3 × 2 cm^3 × 1 cm^3. After that, polished on SiC papers to 2000 grit and subsequently prosperously polishing with 1 μm Al$_2$O$_3$. The amount of martensite for each specimen was examined by XRD on Rigaku. The step was 0.02° min^{-1} over 2θ of 20° to 120°
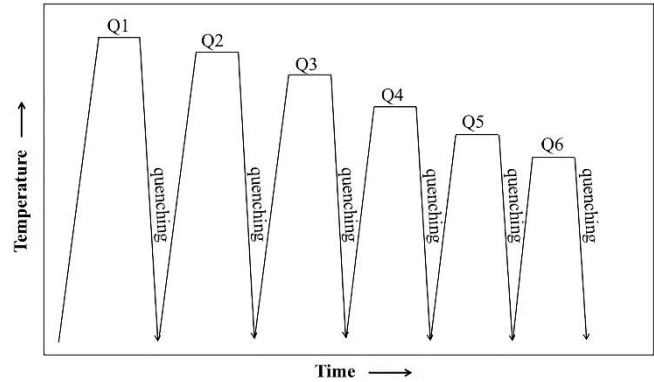

Figure 1. Schematic of multi-step heat treatments processing.

and unfiltered CuKα at 40 kV and 200 mA. The etching applied for scanning electron microscopy (SEM) specimens was 3% Nitric acid volumetric. The morphology and fracture surface were measured on a FEI QUANTA 250.

2.3 Mechanical measurements

Rockwell scale C (HRC) measurements were executed on the unetched samples with a 120-degree diamond cone. The 150 kgf load was pressed into the surface with 15 s of indented time. Ten different interface areas on each example were average. A tension measuring machine was labored out used Hounsfield H10KS. The 50 mm gauge length test samples have corresponded to the standard ASTM E8 circuitous instant.

3. Results and analysis

3.1 Microstructural characterizations

Figure 2(a) presented the x-ray diffraction pattern corresponding to heat treatment of as-sheet, Q1, Q4, Q5, and Q6 heat treatment conditions. The BCC of retaining austenite peak was not overseeding in at all states. The transfiguration of unreformed γ-austenite to bainitic ferrite structure has occurred during the tempered process [10]. The stress field possession reflected in the extensiveness of the XRD peak and intensity. A particular delineation of the prominent peak of (110)$_α$ demonstrates in Figure 2(b). The rise expands, and an abbreviation was encountered in the y-axis intenseness. The height of XRD incurred
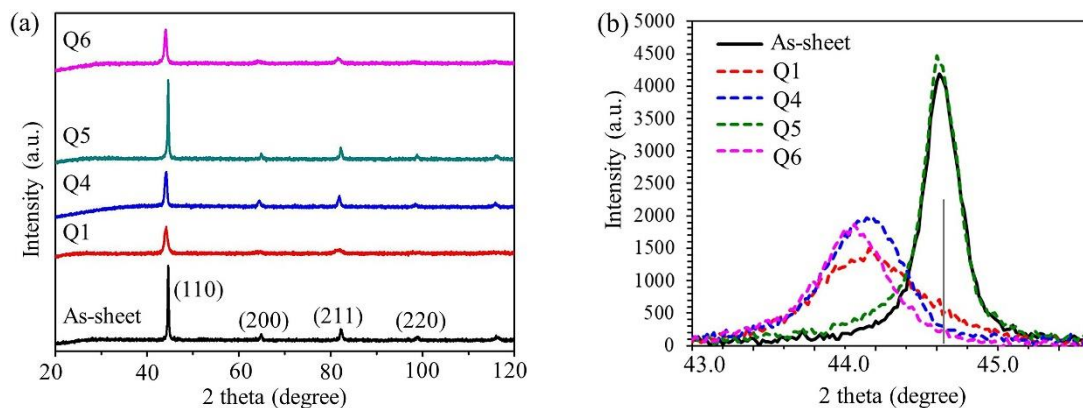

Figure 2. (a) XRD pattern and (b) prominent peak of (110)$_α$.

APICHAI, P.

a peak width increased as the heat treatment step raised liken with the as-sheet condition, with no residual stressed (solid line), as a description of Lozano *et al.* [12], except in Q5 heat treatment condition. The diffraction peak width of Q1, Q4, and Q6 heat treatment conditions were shorter than a half-maximum height of as-sheet condition.

The ferrite–pearlite phase in Figure 3 was well orientated along with the rolling direction of as-sheet condition-the appearance of an originally pearlitic after a periodization heat treatment. The "lamellae" of cementite turned into approximately spherical cementite particles. They minimize the amount of θ/α interfacial area/energy per unit volume. The multi-step contrasting consisted of four different quenching temperatures (Q1, Q4, Q5, and Q6 heat treatment conditions), which were applied to compare the influence on the microstructural and mechanical measurements of 5160 sheets of steel. The processing route to develop martensite microstructures was according to Figure 4-8. The primary step was quenched after enforced austenite matrix by Q1 hardening followed by water, oil, and brine quench. Figure 4 shows a composition pack of parallel late α′-martensite and blocks of plate α′-martensite. A retained austenite introduces a considerably high-carbon alloy after the quenching process [13].

Figure 5 observed an intercritical tempering at 870°C and 840 °C, 30 min (Q2 and Q3) operated to originate an α-ferrite and α′-martensite mixture with a distribution of secondary carbide. And the phase present

was show improve a distribution of secondary carbide by heat treatment step in Q4. The solid solution reduction during hardening treatment was clearly caused by the copper precipitates distribution [14-16]. In the procedure, regarded intercritical tempered treating, elaborate γ-austenite reverted from alloying-rich α′-martensite. That further enriched by partitioning. Nano-sized microalloying compound carbides and Cu continued to precipitation during this process [8]. Cu-rich
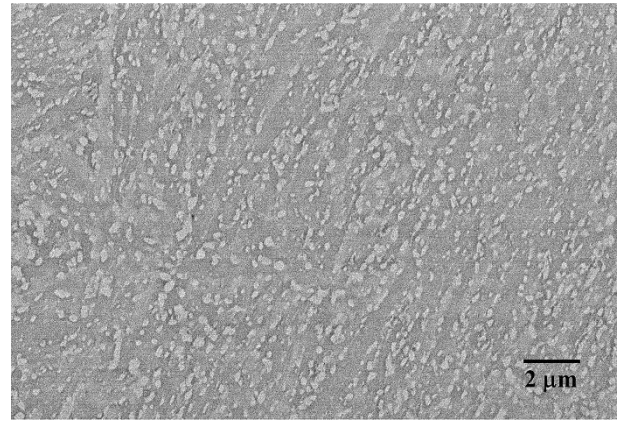
Figure 3. SEM micrographs showing the microstructures of the as-sheet condition by scanning electron microscopy magnification of 20000x.
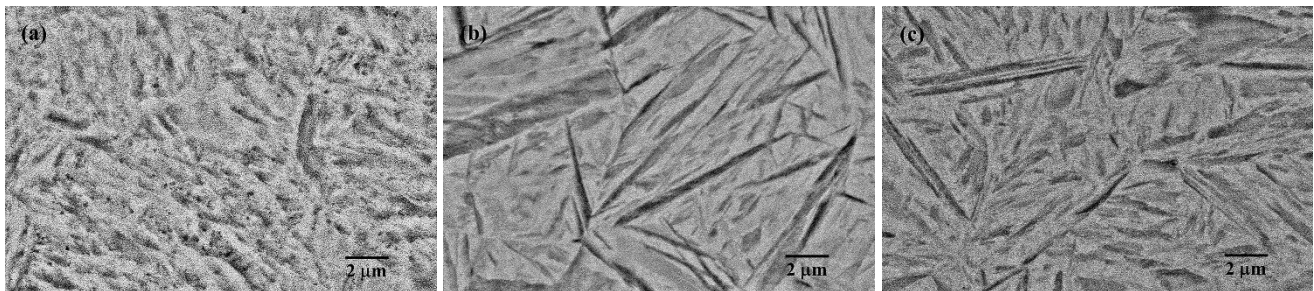
Figure 4. SEM micrographs showing the microstructures after Q1 followed by quenching into (a) water, (b) oil and (c) brine.
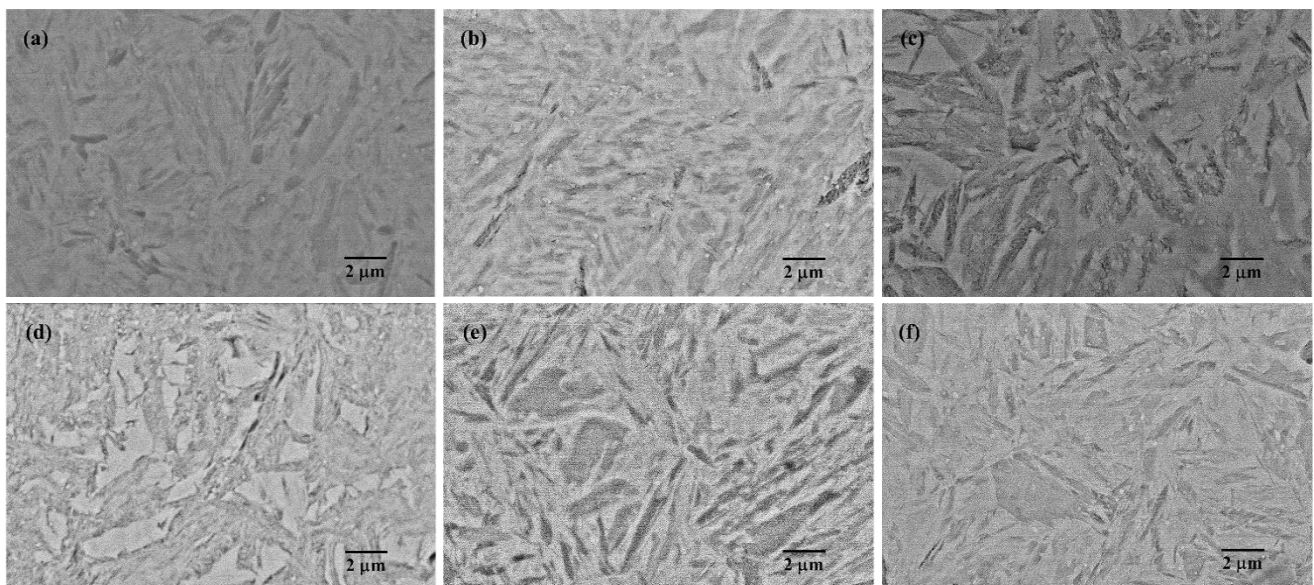
Figure 5. SEM micrographs showing the microstructures after Q2 followed by quenching into (a) water, (c) oil and (e) brine, and Q3 followed by quenching into (b) water, (d) oil and (f) brine.

precipitation was used to strengthen the phase into the tempered martensite. Tempered martensite is newly formed from the metastable austenite in the mixture-phase microstructural. Therefore, precipitated inhomogeneously distributed Cu-rich precipitating in the cubic matrix enhanced the tensile strength of the alloy metal [17-19]. Cu-rich precipitated selective precipitating in metastable γ-austenite. The inflexible tempering α′-martensite was a foreshadowing procurator approach for receding the tensile stress.

Figure 7, the steel sheets were then Q5 hardening into the water, oil, and brine quench to refine the martensite structure to be more plate-like with a distribution carbide. Q5 hardening microstructural comprised dark α-ferrite grain following gray regional phases of tempered-martensite. The martensite substructures were changed during tempering at high temperatures, strongly influenced by an expansive dwindling in dislocation denseness and the absolute recovering of late previous boundary [20]. Transformation accommodation dislocations were procreated by tacking hardening α′-martensite into a softening α-ferrite grain. The conversion was helpful in-store strength hardenability of Fe-C alloying by persuading strain-gradient plasticity, autonomous of the α-ferrite particle size [21-22].

Accordingly, the recrystallizing of α-ferrite was detained, and the microstructural was replaced. In the circumstant of 5160 sheets of steel, the matrix's recrystallization could be retarded by controlling

the identical distribution of the binary compound. Which was also finely dispersed, involving the sub-grain amount carbide/ferrite boundaries. The linear crystallographic defect and the transfusion of irregularity directed to a roughening of the grains. The crystallography non-modulation increased among adjoining grains represented in the adjacent Figure 7(a-c). The interfered quenched experimentation was obtained the pinned result qualified by unmelted binary compound of carbon. The inhibition to deformed grain and grain growth anew formed a γ-austenite contribution [23].

Finally, on the 5160 sheets, some intercritically tempering was executed at 680°C (Q6), Figure 8(a-c), followed by water, oil, and brine quenching. The Q6 heat treatment was expected to improve strength and ductility to accept relatively martensite morphology. The samples were directly connected with the heating Fe blocks for a capable thermal alienate [10]. Following the literature [24], super-saturate solid solutions were significantly in the case. The confines of metastable depended on the excessive intensity and the dissolving solids solution balance. It could demonstrate that excess carbon was an essential auxiliary to the collected potency of α′-martensite. The α′-martensite was not a diffusion-less transformation at low-temperature. The origin α′-martensite structures were conserved. The free energy of dislocation density is owned to the entrapping of C content in α′-martensite as a formality of its C intenseness [25].
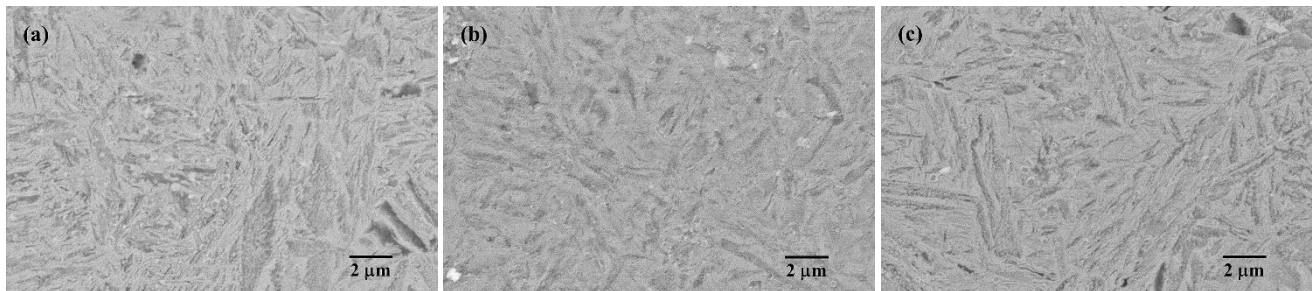
Figure 6. SEM micrographs showing the microstructures after Q4 followed by quenching into (a) water, (b) oil and (c) brine.
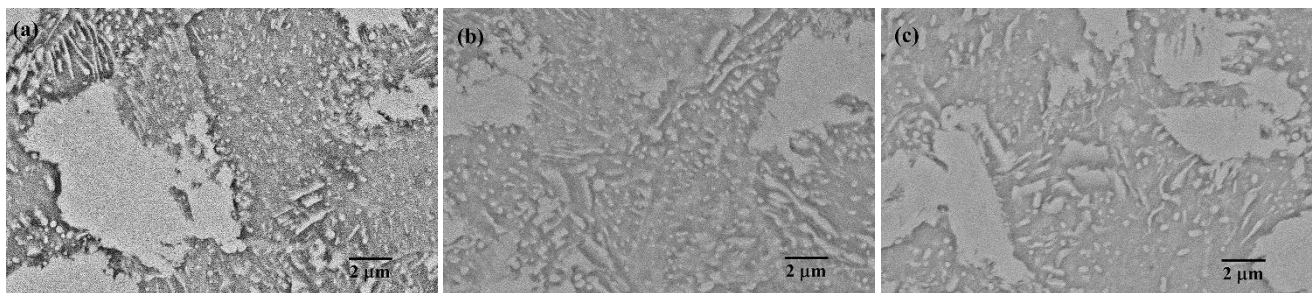
Figure 7. SEM micrographs showing the microstructures after Q5 followed by quenching into (a) water, (b) oil, and (c) brine.
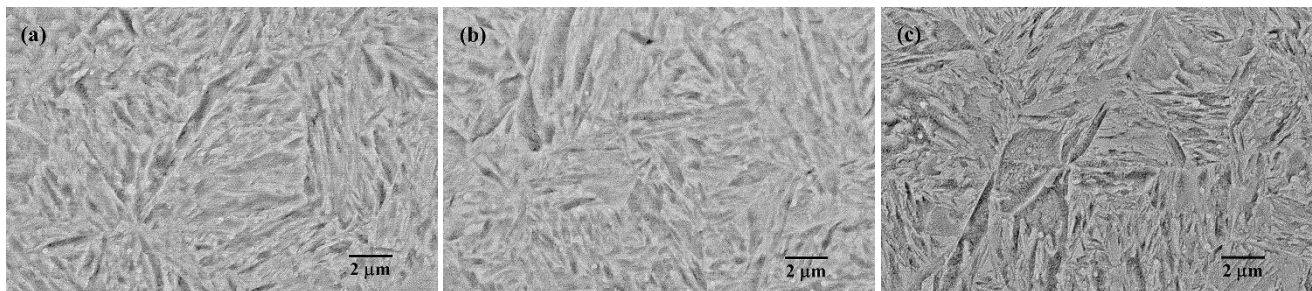
Figure 8. SEM micrographs showing the microstructures after Q6 followed by quenching into (a) water, (b) oil, and (c) brine.

3.2 Mechanical measurements

Figure 9 showed the variation in the heat treatment conditions' Rockwell hardness at room temperature. It could be seen that increased the hardness with increased hardening generation correlated to the as-sheet example. The as-sheet steel was about 40 HRC hardness. After Q1 hardening followed by quenching into the water, oil, and brine, it accomplished the maximum hardness of about 65, 60, and 61 HRC.

It was evident that the hardness early relieved slightly and subsequently rose as the hardening procedure increased from Q2 to Q4 hardening conditions. The average hardness values at Q5 specimens of water, oil, and brine quenching were 26, 24, and 27 HRC, respectively, which presented the coarsening tempered-martensite transformation. Some quenchants on microstructure characterization and mechanical properties have been published in Apichai [16]. Moreover, the hardness tended to increase in hardening at Q6 hardening, followed by quenching into oil, brine, and water because the martensite matrix contains a large amount of secondary carbide.

The ultimate tensile strength and percentage elongations were enumerated in Figure 10 and Figure 11, respectively, to contrast the identity materials of the experiments 5160 sheets after various quenching steps. The ultimate tensile strength and elongation in the as-sheet condition were about 510 MPa and 6.8%, respectively. The Q1 to Q6 hardening greatly influenced the ultimate tensile strength and percentage elongations their varied from 447 MPa to 835 MPa and 4.56% to 13.88%, respectively. The process receded brittle by permanent distortion and ductility crack. Moreover, the coarse phase transformation in the tempering process, which accelerated the ultimate tensile strengths, decreased after Q5 hardening conditions, whereas the percentage elongation increased. After heating at 680℃ (Q6) followed by oil quenching, the maximum stress and elongation were 835 MPa and 12.09%, respectively, which was approximately linear with excellent tensile properties. The result indicated that a bulgy quantity of secondary carbide in the α′-martensite structure induced by inclusions was conducive to improve mechanical properties.

Figure 12 and Figure 13 explored the macro-fractography and FE-SEM image of crack ground of five examples from the tensile test. The fractography was characterized by many cracked features connected with the brittle fracture aspect of the as-sheet condition sample in Figure 12. These transform results into brittle martensite with low toughness were consistent with Liu *et al.* [19].

It was quite notable in Figure 13 that the appearance of the fractured surface involved cleavage facets, tear ridges, and dimples in all of the samples, achieving a signature of integration of ductility fracture and brittleness crack. Figure 13 represented a micrograph of the thin crack interface of the divergent tension specimens. For the as-sheet example in Figure 13(a), the fractured noticeable of a ductility crack was most likely to be observed as a dull and fibrous appearance called dimples. Dimples were featured by the beginning and unification of microvoids round grains. At inherited deformity, the voids expand in volume, and finally, the interconnected tendons of the steels obtained differentiated, producing dimple fracture [10].

After Q1 and Q4 heat treatment, a representative thin crack character grows along the grain boundaries was displayed in Figure 13(b-c).

The metallurgy or control determinants affect the interface between two grains. It became a mushy pathway for cleave generating intergranular-stress crack results. Reproach differentiation, a procession of pits and fractures at higher temperatures disclose, and corrosive grain boundary was the rationale for steels to spoil their strength of bonding crash in a weak-intergranular kind. A characteristic edges of lattices fracture indicated the aspect of fracture generation after Q5 heat treatment, as seen in Figure 13(d). Spontaneous brittleness steels or ductility steels influencing certain physical factors. Intergranular crack phases were other kinds of embrittlement. It developed superficial below definite metallurgy terminations affectation the brittleness of the steels.
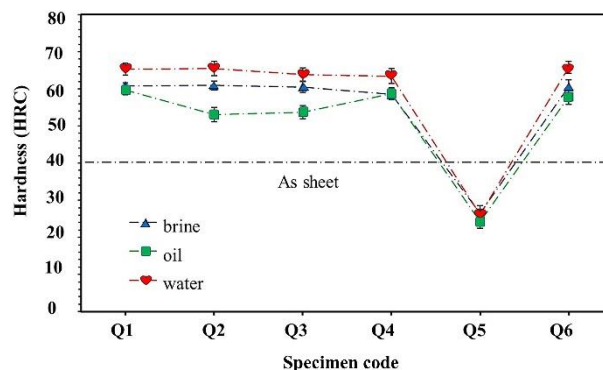

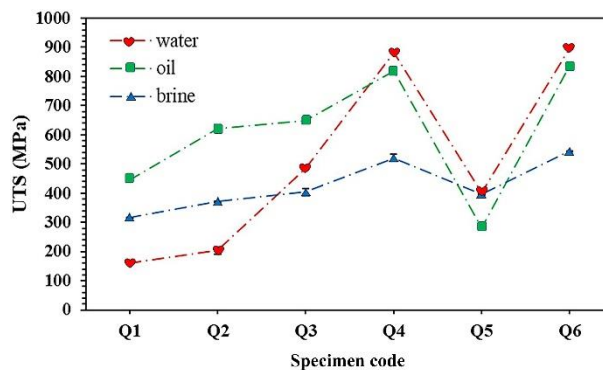**Figure 9.** The hardness after quenching into different heat treatment conditions.

Figure 10. The ultimate tensile strength after quenching into different heat treatment conditions.
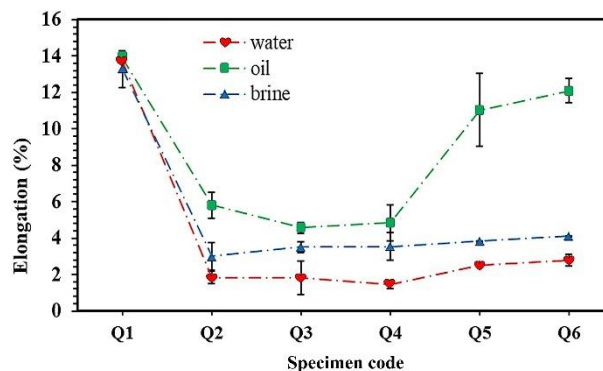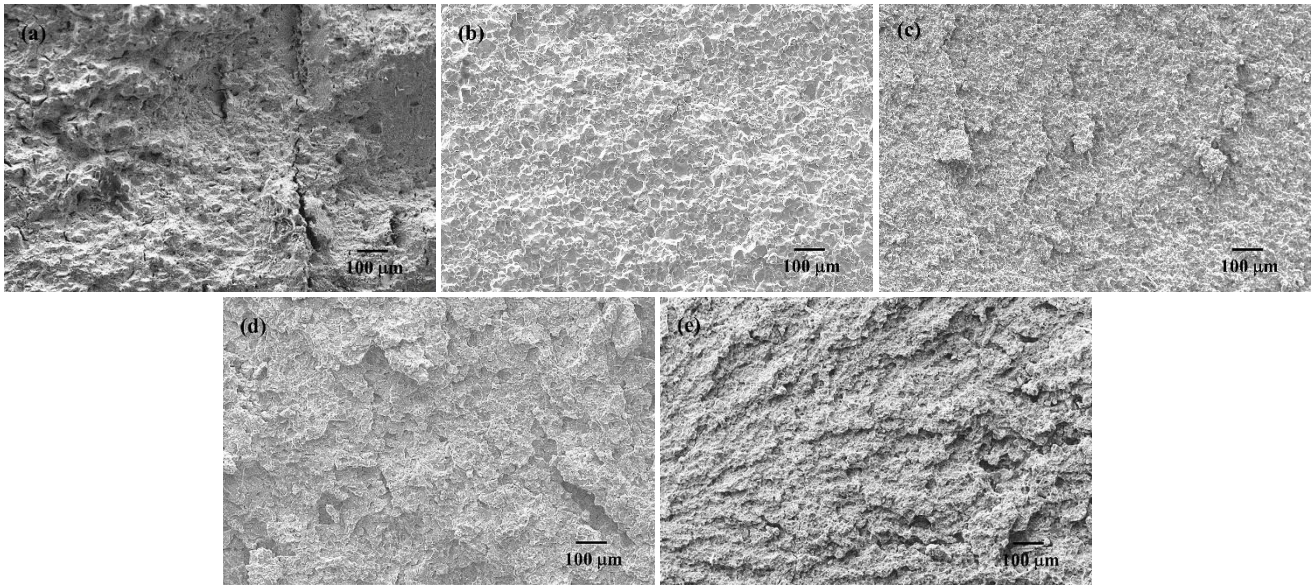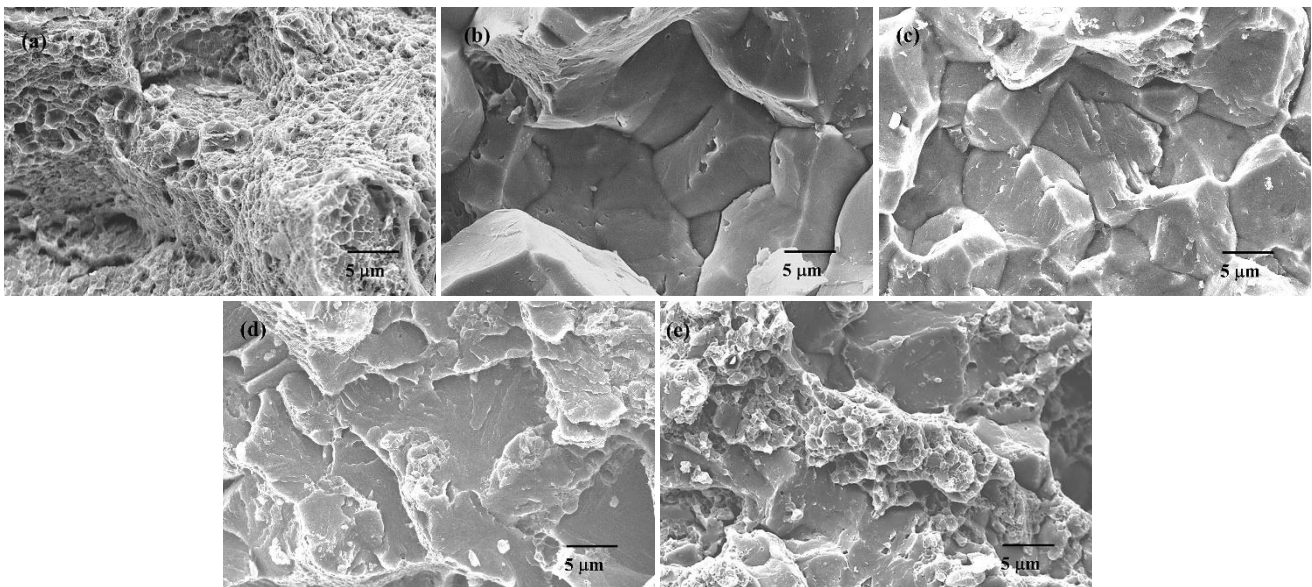

Figure 11. The percentage elongation after quenching into different heat treatment conditions.

Figure 12. Fracture interface in (a) as sheet condition and after (b) Q1, (c) Q4, (d) Q5, and (e) Q6 heat treatment conditions.

Figure 13. Fracture microstructure in (a) as sheet condition and after (b) Q1, (c) Q4, (d) Q5, and (e) Q6 heat treatment conditions.

The micro-crack structure was composed of cleavage fracture and ductile fracture. The primary fracture consisted of a representative river-like surface and tongue's surface [4], identical to the overall percentage elongation of Q6 heat treatment conditions in Figure 13(e). The high elasticity correlated to the enlarged used heat treating procedure reasoned by the γ-austenite to α′-martensite convert during deformity. The hardening process at the beginning reduces and then improves with maintains ductility. The increased heat treatment step procedure achieved the optimized properties of 5160 alloy steel.

4. Conclusions

The heat treatment in 5160 sheets of steel was a development of microstructural, hardness, and strength properties. The multi-step processing consists of six different quenching temperatures used to compare the influence on the morphology evaluation and mechanical applications of 5160 steel. At the lower temperature step treatment, the initial and converted to α′-martensite strength increased with increasing quenching step. The Q4 hardening followed by water, oil, and brine were significant factors influencing the hardness and ultimate tensile strength attributed to carbide distribution in the martensite matrix while decreased the percentage elongation. The strengthening dropped sharply after the Q5 hardening stages of quenching. However, a carbide distribution in tempered martensite matrix after Q6 hardening achieved hardness, ultimate tensile strength, and percentage elongation. In summary, The Q6 hardening was an effective way to develop 5160 steel that causes the optimum combination of strength, percentage elongation, and hardness could be overrun by controlling the prior tempered martensite matrix with a carbide distribution form.

Acknowledgements

References

[1] M. S. Htun, S. T. Kyaw, and K. T. Lwin, "Effect of heat treatment on microstructures and mechanical properties of spring steel," *Journal of Metals, Materials and Minerals*, vol. 18, no. 2, pp. 191-197, 2008.

[2] W. H. Zhou, H. Guo, Z. J. Xie, X. M. Wang, and C. J. Shang, "High strength low-carbon alloyed steel with good ductility by combining the retained austenite and nano-sized precipitates," *Materials Science and Engineering A*, vol. 587, pp. 365-371, 2013.

[3] W. H. Zhou, X. L. Wang, P. K. C. Venkatsurya, H. Guo, C. J. Shang, and R. D. K. Misra, "Structure–mechanical property relationship in a high strength low carbon alloy steel processed by two-step intercritical annealing and intercritical tempering," *Materials Science and Engineering A*, vol. 607, pp. 569-577, 2014.

[4] S. Wang, H. Yu, T. Zhou, L. Wang, "Synergetic effects of ferrite content and tempering Temperature on mechanical properties of a 960 MPa grade HSLA steel," *Materials*, vol. 11, no. 2049, pp. 1-13, 2018.

[5] J. H. Jang, J. Moon, H.-Y. Ha, T.-H. Lee, and D.-W. Suh, "Quantum-mechanical analysis of effect of alloying elements on ε-martensite start temperature of steels," *Scientific Reports*, vol. 7, no 17860, pp 1-11, 2017.

[6] J. Sas, T. Kvačkaj, O. Milkovič, and M. Zemko, "Influence of hot plastic deformation in γ and ($\gamma + \alpha$) area on the structure and mechanical properties of high-strength low-alloy (HSLA) steel," *Materials*, vol. 9, no. 971, pp. 1-8, 2016.

[7] G. Sahoo, K. K. Singh, and V. Kumar, "Quenched and tempered high strength steel: A review," *Journal of Metals, Materials and Minerals*, vol. 30, no. 4, pp. 19-29, 2020.

[8] W. H. Zhou, H. Guo, Z. J. Xie, C. J. Shang, and R. D. K. Misra, "Copper precipitation and its impact on mechanical properties in a low carbon microalloyed steel processed by a three-step heat treatment," *Materials and Design*, vol. 63, pp. 42-49, 2014.

[9] Z.-J. Xie, C.-J. Shang, X.-L. Wang, X.-M. Wang, G. Han, and R.-D.-K. Misra, "Recent progress in third-generation low alloy steels developed under M^3 microstructure control," *International Journal of Minerals, Metallurgy and Materials*, vol. 27, no. 1, pp. 1-9, 2020.

[10] Z. Pan, B. Gao, Q. Lai, X. Chen, Y. Cao, M. Liu, and H. Zhou, "Microstructure and mechanical properties of a cold-rolled ultrafine-grained dual-phase steel," *Materials*, vol. 11, no. 1399, pp. 1-11, 2018.

[11] H. Guo, X. Feng, A. Zhao, Q. Li, and J. Ma, "Influence of prior martensite on bainite transformation, microstructures, and mechanical properties in ultra-fine bainitic steel," *Materials*, vol. 12, no. 527, pp. 1-15, 2019.

[12] D. E. Lozano, G. E. Totten, Y. Bedolla-Gil, M. Guerrero-Mata, M. Carpio, and G. M. Martinez-Cazares, "X-ray determination of compressive residual stresses in spring steel generated by high-speed water quenching," *Materials*, vol. 12, no. 1154, pp. 1-11, 2019.

[13] Q. Luo, "A new XRD method to quantify plate and lath martensites of hardened medium-carbon steel," *Journal of Materials Engineering and Performance*, vol. 25, no. 6, pp. 2170-2179, 2016.

[14] H. L. Yi, K. Y. Lee, and H. K. D. H. Bhadeshi, "Mechanical stabilisation of retained austenite in δ-TRIP steel," *Materials Science and Engineering A*, vol. 528, pp. 1-9, 2011.

[15] A. Stormvinter, A. Borgenstam, and P. Hedström, "Investigation of lath and plate martensite in a carbon steel," *Solid State Phenomena*, vol. 172-174, pp. 61-66, 2011.

[16] P. Apichai, "Effects of quenchants on microstructures and mechanical properties of steel grade AISI 5160," *Journal of Metals, Materials and Minerals*, vol. 30, no. 3, pp. 15-23, 2020.

[17] C. G. Andrès, G. Caruana, and L. F. Alvarez, "Control of $M_{23}C_6$ carbides in 0.45C-13Cr martensitic stainless steel by means of three representative heat treatment parameters," *Materials Science and Engineering A*, vol. 241, no. 1-2, pp. 211-215, 1998.

[18] A. F. Candelária, and C. E. Pinedo, "Influence of the heat treatment on the corrosion resistance of the martensitic stainless steel type AISI 420," *Journal of Materials Science Letters*, vol. 22, pp. 1151-1153, 2003.

[19] W. Liu, Y.-H. Jiang, H. Guo, Y. Zhang, A.-M. Zhao, and Y. Huang, "Mechanical properties and wear resistance of ultrafine bainitic steel under low austempering temperature," *International Journal of Minerals, Metallurgy and Materials*, vol. 27, no. 4, pp. 483-493, 2020.

[20] V. H. B. Hernandez, S. S. Nayak, and Y. Zhou, "Tempering of martensite in dual-phase steels and its effects on softening behavior," *Metallurgical and Materials Transactions A*. vol. 42A, pp. 3115-3129, 2011.

[21] Y. I. Son, Y. K. Lee, K. T. Park, C. S. Lee, and D. H. Shin, "Ultrafine grained ferrite–martensite dual phase steels fabricated via equal channel angular pressing: microstructure and tensile properties," *Acta Materialia*, vol. 53, pp. 3125-3134, 2005.

[22] K. T. Park, Y. K. Lee, and D. H. Shin, "Fabrication of ultrafine grained ferrite/martensite dual phase steel by severe plastic deformation," *The Iron and Steel Institute of Japan International*, vol. 45, pp. 750-755, 2005.

[23] R. Ding, D. Tang, A. Zhao, H. Guo, J. He, and C. Zhi, "Effect of ultragrain refinement on quenching and partitioning steels manufactured by a novel method," *Materials and Design*, vol. 87, pp. 640-649, 2015.

[24] A. F. Brust, S. R. Niezgoda, V. A. Yardley, and E. J. Payton, "Analysis of misorientation relationships between austenite parents and twins," *Metallurgical and Materials Transactions A*, vol. 50, pp. 837-855, 2019.

[25] A. Turk, G. R. Joshi, M. Gintalas, M. Callisti, P. E. J. Rivera-DÃ-az-del-Castillo, and E. I. Galindo-Nava, "Quantification of hydrogen trapping in multiphase steels: part I - point traps in martensite," *Acta Materialia*, vol. 194, pp. 118-133, 2020.